Method of GIS Background Subtraction

Y.Ikebe, Y.Ishisaki, H.Kubo, E.Idesawa, T.Takahashi, K.Makishima
and GIS team

May 24, 1995

1 Introduction

To estimate the background precisely is one of the key issues with the analysis of spatially extended emissions, such as clusters, because the background increases roughly in proportion to the area on the focal plane to be used. Particularly at the outer fainter parts of the target source, the background flux often becomes comparable to, or even larger than, the source signal.

The background consists of the Non-X-ray Background (NXB) and Cosmic X-ray Background (CXB). The NXB may in principle be *predicted* based on relevant set of information, such as the GIS monitor counts and the satellite position at the time of data acquisition. However such a background simulator is still under development. One immediate solution to the issue is to use the actual data from blank sky fields which includes both NXB and CXB.

In section 2 we will briefly review the GIS background characteristics. In section 3 we describe the most up-to-date method to estimate the background at a specified region on the detector. The systematic uncertainty with this method will be discussed in section 4.

2 Characteristics of the NXB and CXB components

As already described in Kubo et al. (ASCA News No.2), the NXB count rate depends mainly on the position on the detector and COR (cutoff rigidity) along the satellite orbit. The NXB count rate depends strongly on COR (Fig.1), while the NXB brightness is not quite symmetric around the detector center (Fig.3 in "ASCA Medium Sensitive Survey with GIS, Ishisaki et al." in this issue) .

For typical observations, a significant fraction of exposure is made over a COR range of 10-14 GeV/c where the NXB count rate depends little on the COR. Actually as shown in Fig.2, for COR $>$ 10 GeV/c the NXB counts rate is constant within 30%.

In the COR range of 11-12 GeV/c, we sometimes (typically once a day) observe flare-like events in which the NXB count rate significantly increases for about 10 minutes. These events are of terrestrial origin, because they occur preferentially when the space

craft is near the south-Atlantic anomaly (Fig.3). Although the origin of these events are yet to be identified, they can be eliminated by applying a longitude-latitude discrimination in reference to Fig.3.

In contrast to the NXB, the CXB intensity and spectrum can be regarded as almost constant all over the sky at least for our purpose. However, because of the XRT vignetting, the CXB intensity observed on the detector decreases with the distance from the XRT optical axis. The CXB brightness has an approximate circular symmetry on the focal plane. However in the GIS field, the circular symmetry in the CXB brightness is violated by partial shadows of the GIS window support grids.

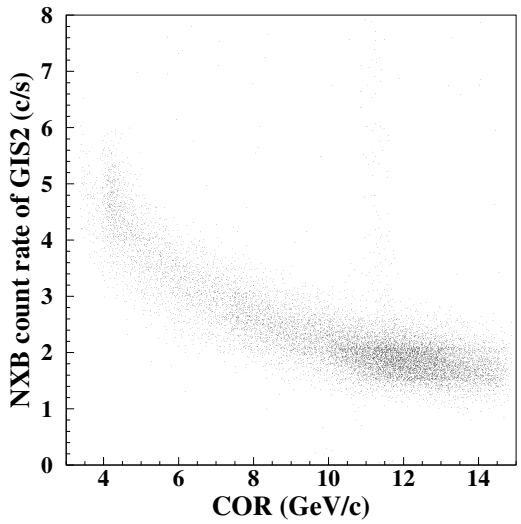

Figure 1: Correlation between the GIS *L1* count (one of the monitor words) and the cutoff rigidity (COR) for cosmic rays. Each data point is an average every 32 second interval. Note that the *L1* counts include the ~ 0.3 c/s X-ray events from the calibration isotope, as well as events which will be eliminated by the CPU-based on-board spread discrimination and by the on-ground rise-time discrimination with GIS_CLEAN. Finally uneliminated-NXB count rate is ~ 0.2 c/s.

3 Background subtraction methods

3.1 A direct subtraction of blank sky photons

To a rough approximation, we can construct the background for any specified region on the detector plane using the actual data of blank sky fields. During the PV-phase, totally 15 separate pointings onto blank skies have been performed on three different sky regions (NEP, QSF3, and DRACO). The GIS mode during these observations is mostly the standard one, i.e. the same as is used for a majority of guest observations. By summing up all these available blank sky data, we can construct the GIS background with good statistics.

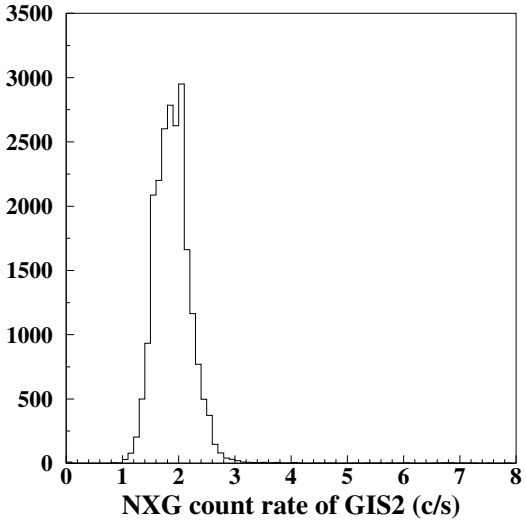

Figure 2: Distribution of NXB count rate when COR $>$ 10 GeV/c.

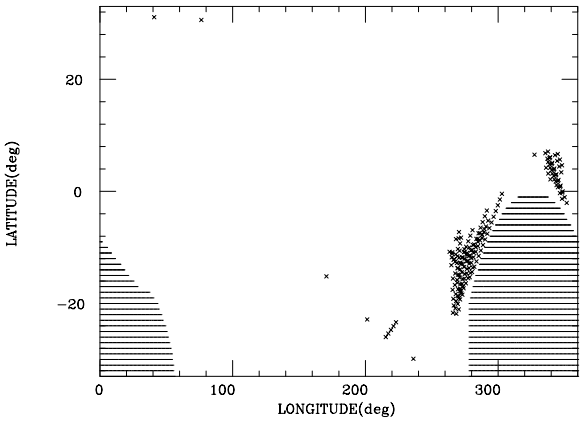

Figure 3: Histogram of the satellite longitudes and latitudes when the flare-like events are detected. The shaded area corresponds to the south-Atlantic anomaly.

These blank sky data has already been made publicly available in the form of several photon files, as sorted every 2 GeV/c step in the COR ranges. Because the NXB depends on COR, it seems to be a good idea to sort the on-source spectra into the same COR ranges as the background photon files, and subtract the corresponding background. We recommend the users to limit the COR range to $>$ 10 GeV/c in the data analysis, and use the background accumulated for the same COR range from the background photon files.

3.2 An improved method

Strictly speaking, the blank sky data include faint sources which may be bright enough for some purpose. At a flux level of 1×10^{-13} ergs s^{-1} cm^{-2} which is an approximate

limiting sensitivity of the GIS, we expect on the average a few sources per GIS field of view. In fact, in the north ecliptic pole (NEP) field, we can immediately recognize two X-ray sources (Fig.4). One of them, NGC6552 (Fukazawa et al. PASJ 46,L141,1994), is bright and hard enough to influence the mean background spectrum at that position.

By taking these faint sources into account, we have developed an improved method of GIS background subtraction. We pick up all the possible faint sources in each blank-sky image, and discarded photons which fall close to them. The background photon information thus processed will be released as Masked Blank sky Event File (MBEF). Below we describe how the MBEF has been generated and how it is to be used.

The method to find the possible faint sources in a GIS image has been investigated by the MSS project team (Ishisaki et al. in this issue). In short, an GIS image is fitted with a 2-dimensional brightness model constructed from the night Earth image and the day Earth image. The residual image is smoothed with an analytic approximation for the point spread function of the XRT (Fig.5-a), and the distribution of pixel counts is derived as illustrated in Fig.5-b. By fitting the histogram with a Gaussian, we find the distribution mean and an equivalent one sigma, and set the source detection threshold at the 2.5 σ level above the distribution mean. We then make a mask image, which takes a value of 0 where the faint source is present, or 1 where the image is free from faint sources. An example of mask image is shown in Fig.6.

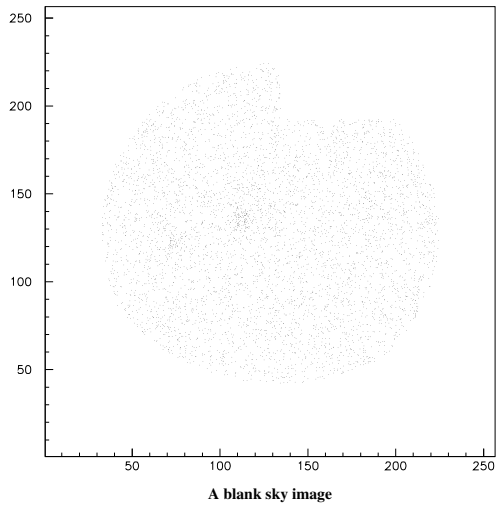

Figure 4: GIS S2 image of the NEP field. The region where the calibration isotope is attached is removed from the image.

We have thus obtained mask images for each individual pointing onto the blank sky, from which we have constructed the Masked Blank sky Event File (MBEF) that was mentioned above. MBEF combines all the photons from the original 15 blank sky pointings, but excluding those events that fall on the masked regions of respective images. We can also define the position-dependent exposure time as

$$Exposure\ Time\ at\ (j,k) = \sum_i T_i \times mask_i(j,k) \qquad (1)$$

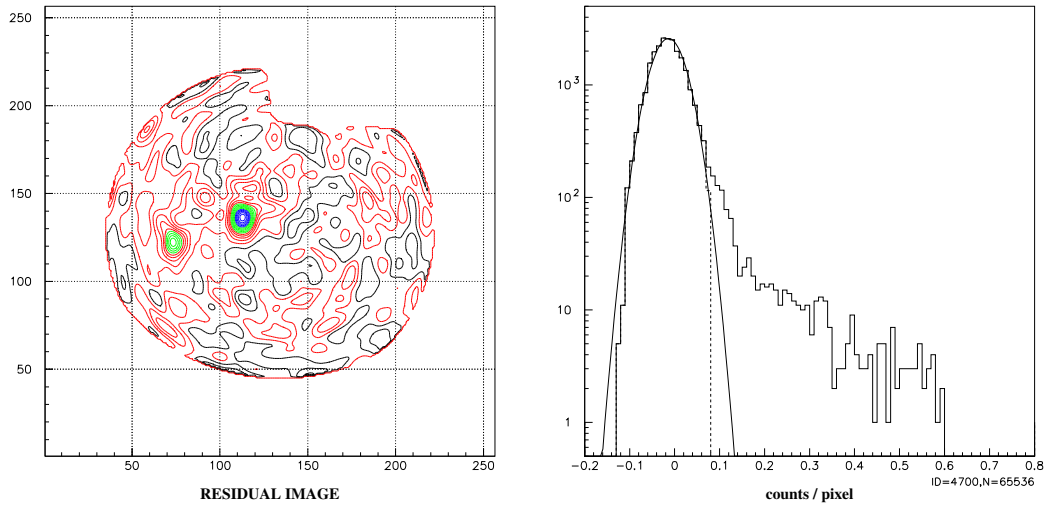

Figure 5: (a)An example of residual GIS image after removing a 2-dimensional template profile, and then smoothed with an analytically approximated PSF. (b)Distribution of pixel count rate in the smoothed residual image, fitted with a Gaussian.

where $i = 1, , , 15$ is the pointing number, T_i is the exposure time of the $i\text{-}th$ pointing, and $mask_i(j,k)$ is the mask file for the $i\text{-}th$ pointing.

When we want to subtract background from the on-source spectrum accumulated over a certain region on the focal plane, we accumulate photons in the MBEF over the same region. After correcting for the position-dependent exposure time, the background spectrum thus accumulated is directly subtracted from the on-source spectrum. In a similar way, we can subtract the background from the observed surface brightness profiles. The MBEF, together with the exposure map calculated with eq.(1), will be released to the guest observers.

4 GIS background reproducibility

Since the background photon files contain a large number of events, the overall uncertainty in the background-subtracted spectrum is dominated either by statistical fluctuations in the on-source data, or systematic error in the background subtraction procedure. Then how good is the NXB reproducibility in the GIS instrument? As already noticed in Fig.2, the instantaneous GIS background varies up to 30 % even for COR > 10 GeV/c, but the variation occurs mostly on time scales of $10 - 30$ minutes. Since the source spectrum is usually accumulated for much longer times, these fluctuations tend to average out and the effective background reproducibility is expected to be considerably better.

This issue may be studied more quantitatively by comparing the overall GIS count rates among the 15 blank sky pointings. However the raw GIS counts simply integrated over the entire GIS field would not be appropriate for this comparison, since they are affected by the presence of faint sources. Therefore we again fitted each blank-sky image

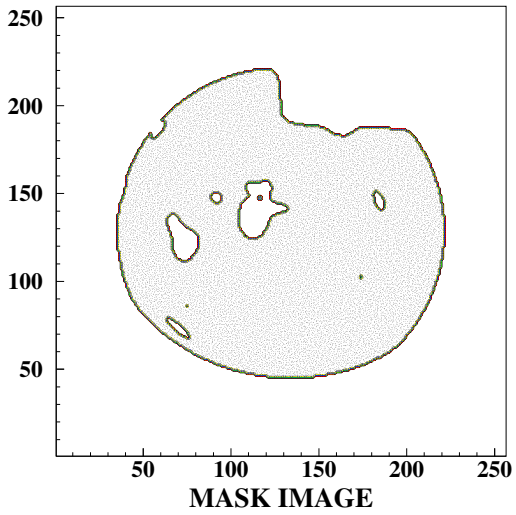

Figure 6: An obtained mask image.

with the two dimensional brightness template, but discarding those regions in each field where the faint sources have been detected. Then the template normalization will serve as a good measure of the background (CXB plus NXB) level for each field. As illustrated in Fig.7, the mean count rates thus estimated exhibit about 2.9% and 3.2% RMS scatter among the 15 fields, for S2 and S3, respectively. Therefore we conservatively quote the systematic error in the GIS background as 4% for both S2 and S3, which corresponds to about 3×10^{-7} counts s^{-1} arcmin^{-2} keV^{-1}.

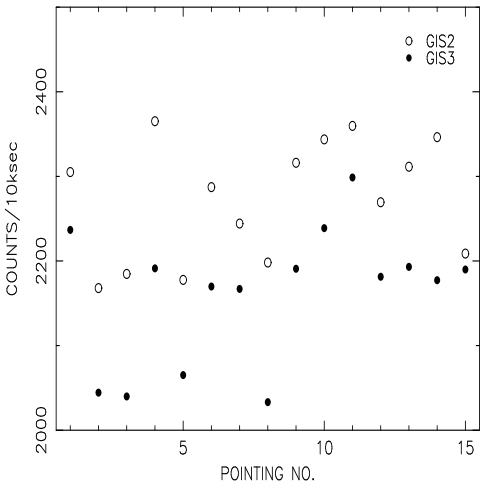

Figure 7: The average count rate of the 15 blank sky observations, as determined by discarding faint sources and fitting the image with a two dimensional brightness template.